



On-Surface Modification of Copper Cathodes by Copper(I)-Catalyzed Azide Alkyne Cycloaddition and CO₂ Reduction in Organic Environments

Ryota Igarashi, Ryuji Takeuchi, Kazuyuki Kubo, Tsutomu Mizuta and Shoko Kume*

Department of Chemistry, Graduate School of Science, Hiroshima University, Higashihiroshima, Japan

In this study, organic structures were introduced onto copper cathodes to induce changes in their electrocatalytic CO₂ reduction activity. Poorly soluble organic polymers were distributed onto the copper surface as a thin layer by polymerizing monomeric precursors *via* a copper(I)-catalyzed azide-alkyne cycloaddition (CuAAC) activated by anodization of the copper substrate. The resulting structure possesses copper surface atoms that are available to participate in the CO₂ reduction reaction—comparable to close-contact organic structures—and stabilize the adsorption of organic layers through the CO₂ reduction process. The CO₂ reduction performance of the on-surface modified copper cathode exhibited improved CO₂ reduction over H₂ evolution compared with traditional cast modification systems. Preventing organic moieties from forming densely packed assemblies on the metal surface appears to be important to promote the CO₂ reduction process on the copper atoms. The suppression of H₂ evolution, a high methane/ethylene ratio, and the influence of stirring demonstrate that the improved CO₂ reduction activity is not only a result of the copper atom reorganization accompanied by repeating anodization for modification; the organic layer also apparently plays an important role in proton transfer and CO₂ accumulation onto the copper surface.

Keywords: CO₂ reduction, copper cathode, CuAAC, organic modification, hydrocarbons

OPEN ACCESS

Edited by:

Hitoshi Ishida,
Kitasato University, Japan

Reviewed by:

Enrico Andreoli,
Swansea University, United Kingdom
Tomohiko Inomata,
Nagoya Institute of Technology, Japan

*Correspondence:

Shoko Kume
skume@hiroshima-u.ac.jp

Specialty section:

This article was submitted to
Inorganic Chemistry,
a section of the journal
Frontiers in Chemistry

Received: 30 January 2019

Accepted: 26 November 2019

Published: 17 December 2019

Citation:

Igarashi R, Takeuchi R, Kubo K,
Mizuta T and Kume S (2019)
On-Surface Modification of Copper
Cathodes by Copper(I)-Catalyzed
Azide Alkyne Cycloaddition and CO₂
Reduction in Organic Environments.
Front. Chem. 7:860.
doi: 10.3389/fchem.2019.00860

INTRODUCTION

The reduction of CO₂ on metal copper cathodes has been of interest since it was first reported by Hori in 1985 (Hori et al., 1985, 1986). The specific character of copper allows highly reduced hydrocarbons to be obtained at relatively large negative potentials, unlike other catalysts, which mainly afford formate and CO (Gattrell et al., 2006; Peterson and Nørskov, 2012; Zhang et al., 2014; Feaster et al., 2017).

Since common polycrystalline copper surfaces can yield various types of hydrocarbons, product distribution is difficult to control, especially for the selective formation of valuable C2-C3 products such as ethylene and ethanol. Product distribution is known to be highly influenced by the applied potential (Hori et al., 2003; Gattrell et al., 2006; Kuhl et al., 2012), Cu crystal facet (Hori et al., 2003; Gupta et al., 2006; Schouten et al., 2012; Huang et al., 2017; Qiu et al., 2017), and proton transfer conditions (Hori et al., 1997; Singh et al., 2016; Varela et al., 2016; Ooka et al., 2017). Oxide-derived Cu nanostructures are of current interest (Kas et al., 2014; Ren et al., 2015; Dutta et al., 2016; Handoko et al., 2016; Mistry et al., 2016; Huang et al., 2017; Mandal et al., 2018); however, their

high C2-C3 selectivity has not been fully elucidated, as these materials typically include multiple Cu facets endowing various activities. Furthermore, their nano-scale morphology influences local pH, and the remaining oxygen atoms are considered to influence the electronic nature of the surface. Other nanostructured Cu materials synthesized *via* various preparation methods (Tang et al., 2011; Li and Kanan, 2012; Reske et al., 2014; Ma et al., 2015; Kim et al., 2017; Zhao et al., 2017; Jeon et al., 2018; Luna et al., 2018) and alloys comprising copper and other elements are reported to show excellent performance in C2-C3 product formation (Long et al., 2017; Ma et al., 2017; Zhang et al., 2017).

The introduction of organic structures onto catalytically active metal surfaces has recently received attention, particularly the preparation of self-assembled monolayers (SAMs). Traditionally, the adsorption of organic molecules has been used to deactivate pristine metal surfaces and is often exploited to achieve higher selectivity, as demonstrated by the Lindlar catalyst. Recent developments have shown that organic molecules have a positive impact on enhancing selectivity and activity (Schoenbaum et al., 2014). Regarding CO₂ reduction, several groups have introduced organic molecules onto copper surfaces as SAMs to improve the reaction selectivity of CO and CO₂ reduction (Xie et al., 2016; Gong et al., 2017; Ahn et al., 2018). In these studies, phase-separated and densely packed structures of organic molecules on metal surfaces are carefully avoided, and the design of open-surface metal centers with neighboring organic structures to allow their cooperation seems to be a prerequisite for a productive reaction environment. To obtain the right reaction environment, similar to coordination catalysts, in which vacant metal centers can cooperate with organic ligands, requires that specific strategies be adopted in relation to contact-surface preparation.

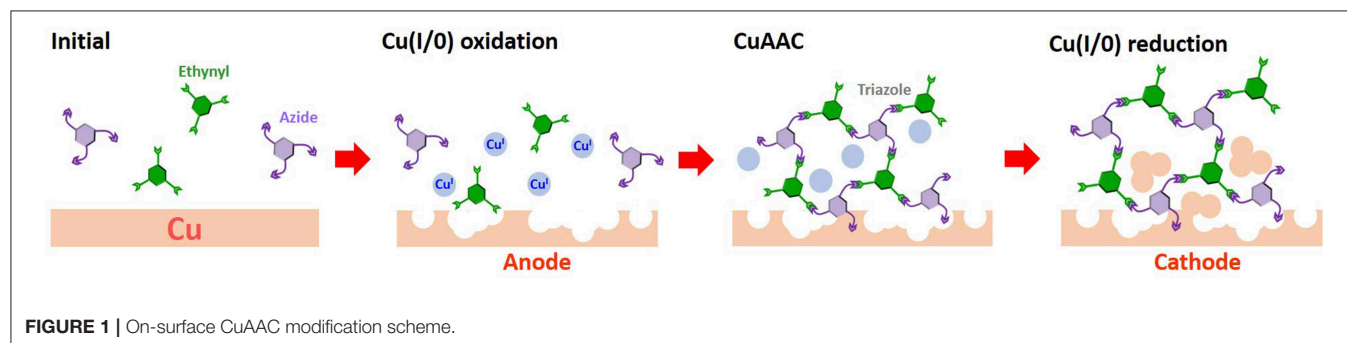
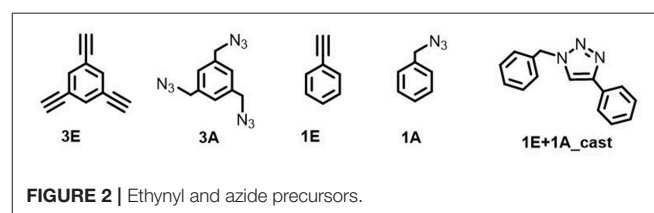
Herein, we have developed a new method to modify metallic copper cathodes with organic layers, in contrast to SAM adsorption routes. To place open metal surface atoms in the neighborhood of the organic structure and to enhance stability, we adopted a rigid organic polymer structure. These polymers are poorly soluble in common solvents and are difficult to distribute homogeneously on the surface without aggregation. To distribute the polymer structure across the surface as a thin layer, the monomeric precursors were polymerized on the copper electrode by exploiting the Cu(I)-catalyzed azide-alkyne

cycloaddition (CuAAC) catalytic activity response to surface oxidation (Figure 1). In this report, the copper modification achieved *via* the on-surface CuAAC approach was studied, and an efficient CO₂ reduction activity, specific to the polymer-modified electrode, was observed.

LAYER PREPARATION AND CHARACTERIZATION

Preparation

Electrochemical on-surface modification was performed in an electrolyte solution containing ethynyl and azide monomers (Figure 2). The redox activity of the surface copper was observed by repetitive anodic scanning of the polycrystalline copper electrode. In the absence of organic additives, the dissolution of oxidized copper from the surface proceeded continuously with an onset potential of *ca.* -0.6 V (Figure 3A). The first anodic scan exposed a fresh surface, making the current double afterward, and the anodic current profile was constant without decrease in the subsequent scans. When 1E or 3E was present in the solution, the onset potential of the copper anodization shifted positively, indicating that the ethynyl moieties promoted adsorption on the copper surface and thus inhibited copper stripping (Figures 3B–E). The appearance of a negatively shifted cathodic peak at *ca.* -1 V indicates coordination of the dissolved copper ion species. The ethynyl moiety likely formed insoluble coordination polymers with copper(I) through sigma- and pi-coordination bonds (Abrantes et al., 1984), and the anodic scanning appeared to first dissolve the copper(I) species into the solution (Ahrland, 1982), with subsequent coordination of ethynyl moieties. When azide precursors coexisted, these peaks were less recognizable (Figures 3B,D), implying that ethynylcopper(I) was consumed in the subsequent CuAAC



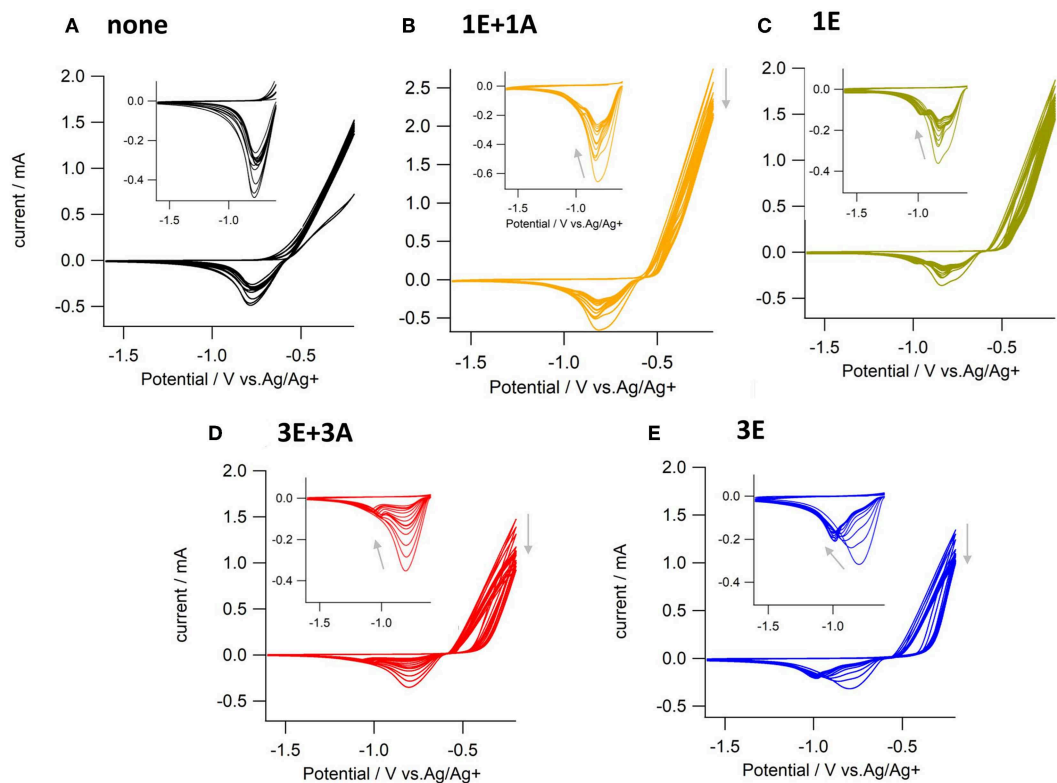


FIGURE 3 | Cyclic voltammograms of copper electrodes scanned 15 times in electrolyte solution containing (A) no additives, (B) 1E and 1A, (C) 1E, (D) 3E and 3A, and (E) 3E. Electrolyte solution; 0.1 M ⁿBu₄NPF₆-acetonitrile, scan rate; 0.1 Vs⁻¹.

reaction. Upon scanning, the anodic current gradually decreased, and an anti-corrosive growth layer was observed on the surface. The current decrease was prominent in 3E+3A, and to a smaller degree, when the solution contained 3E, 1E alone or 1E+1A. The covalent polymers composed of 3E+3A, via the CuAAC reaction, appear to induce strong adsorption compared with 3E without covalent bond formation. The anodic scanning of 1E+1A is expected to afford monomeric 1,2,3-triazoles because they contain only one reaction point for each, resulting in very weak adsorption. These features show that the anticorrosive layer efficiently covered the Cu surface by anodization with 3E+3A.

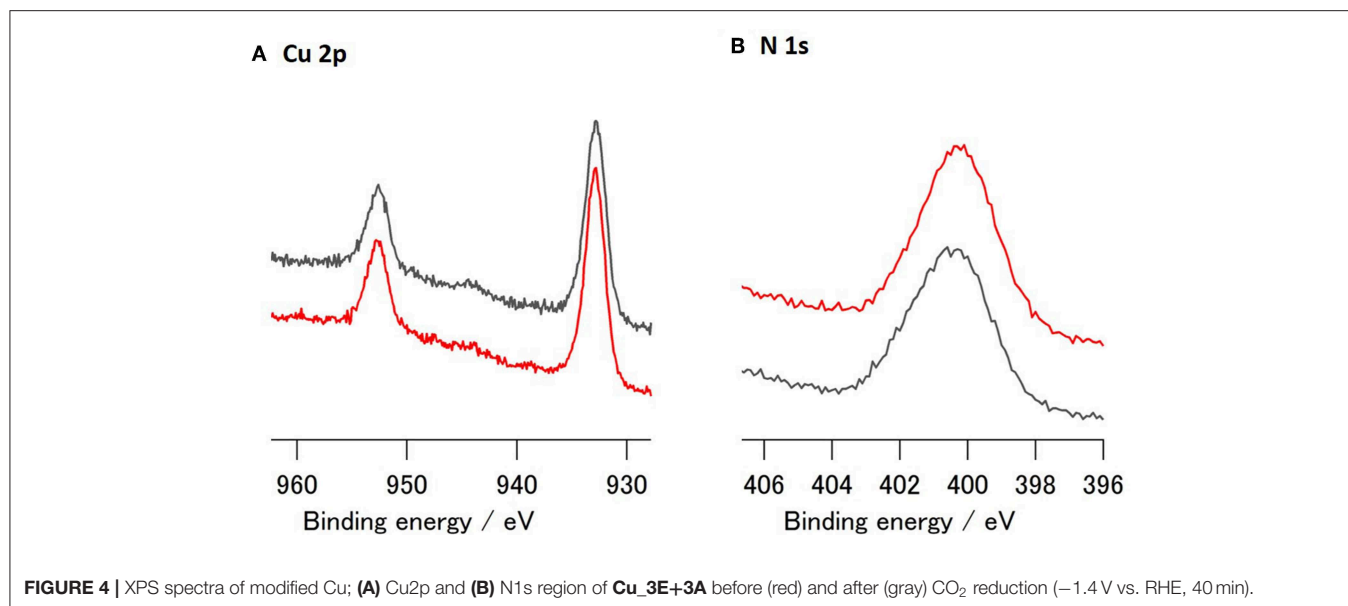
X-Ray Photoelectron Spectroscopy (XPS)

XPS analysis of the Cu_{3E+3A}-modified Cu surface showed that a fair amount of nitrogen was introduced onto the surface (Figure 4). The binding energy associated with the introduced N species does not indicate an azide moiety, as this exhibited a peak located at ~405 eV (Collman et al., 2006; Chisholm et al., 2016). The majority of the nitrogen, when affixed to the surface, appeared in the form of a triazole. Conversely, in addition to the Cu 2p peaks, Cu_{1E+1A} also exhibited a small nitrogen peak upon modification (Figure S1). These nitrogen features correspond to the difference in adsorption of polymeric and monomeric structures, as discussed in the on-surface preparation section,

showing a significant and robust organic modification in polymeric Cu_{3E+3A}.

Scanning Electron Microscopy (SEM)

During the on-surface preparation, a significant amount of grain structures grew from an initially smooth polished Cu polycrystal surface (Figure 5). Additionally, the structures of Cu_{3E+3A}, Cu_{1E+1A}, and Cu_{1E} were similar. Anodic scans of the copper surface result in dissolution and re-deposition of Cu⁺ in acetonitrile in the presence of phenylacetylene, and insoluble copper phenylacetylide is introduced as a stable intermediate (Ahrland, 1982). The grain structures seemed to grow through an oxidation–coordination–reduction process in repetitive anodization cycles, similar to the preparation of copper nanostructures derived from copper oxide CO₂-reduction catalysts. When the number of scan cycles was reduced to seven, the surface was covered by a smaller structure in the early stage of growth (Figure S2). XPS showed that Cu_{3E+3A} contained a higher amount of organic groups on its surface than Cu_{1E+1A}. However, these structures had very similar appearances, implying that the organic moieties were uniformly dispersed on copper grains. The thickness of the rough surface structure is estimated to have been hundreds of nanometers from the cross-sectional SEM image (Figure S3). When molecular triazole was cast on the copper surface (Figure 5E), platelet crystals were formed on the surface.



Additionally, the basal copper itself was observed to be slightly roughened by casting (**Figure S4**), as discussed in the roughness factor section.

Roughness Factor

The roughness of the electrodes was calculated from the double-layer capacitance (**Figure S5**, **Table S1**). **Table 1** details the roughness factors of the Cu electrodes, with the unmodified electrode as the reference. **Cu_1E+1A** and **Cu_1E** exhibited a high degree of roughness, which is consistent with the apparent surface topology observed in the SEM micrographs. Despite the apparent granular morphology, the roughness of **Cu_3E+3A** was similar to that of the smooth unmodified electrode. The surface of the Cu electrode may have been partially insulated by the presence of a thick organic layer film. When the triazole molecule was cast onto the surface, the surface area slightly increased, although no anodization of the copper was achieved. The adsorption of densely packed triazole, and the subsequent cathodization, may result in the re-construction of the surface copper (Gunathunge et al., 2017), as observed in the SEM micrographs.

Underpotential Deposition (UPD)

The amount of exposed Cu atoms on the electrode surface was estimated by UPD analysis (**Figure 6**). There were fewer exposed Cu atoms in the **Cu_3E+3A** electrode than estimated on the basis of the SEM micrograph and roughness factor. The surface of **Cu_3E+3A** is considered to have been largely covered by the organic layer, which inhibited the approach and deposition of Pb²⁺; however, the system maintained its function as an electrode, as the layer could almost be considered as a monolayer in terms of thickness (Bandyopadhyay et al., 1998; Feng et al., 2017). The size of the redox wave was significantly larger in **Cu_1E+1A**, as the monomeric triazole was not able to strongly adsorb onto the surface. Furthermore,

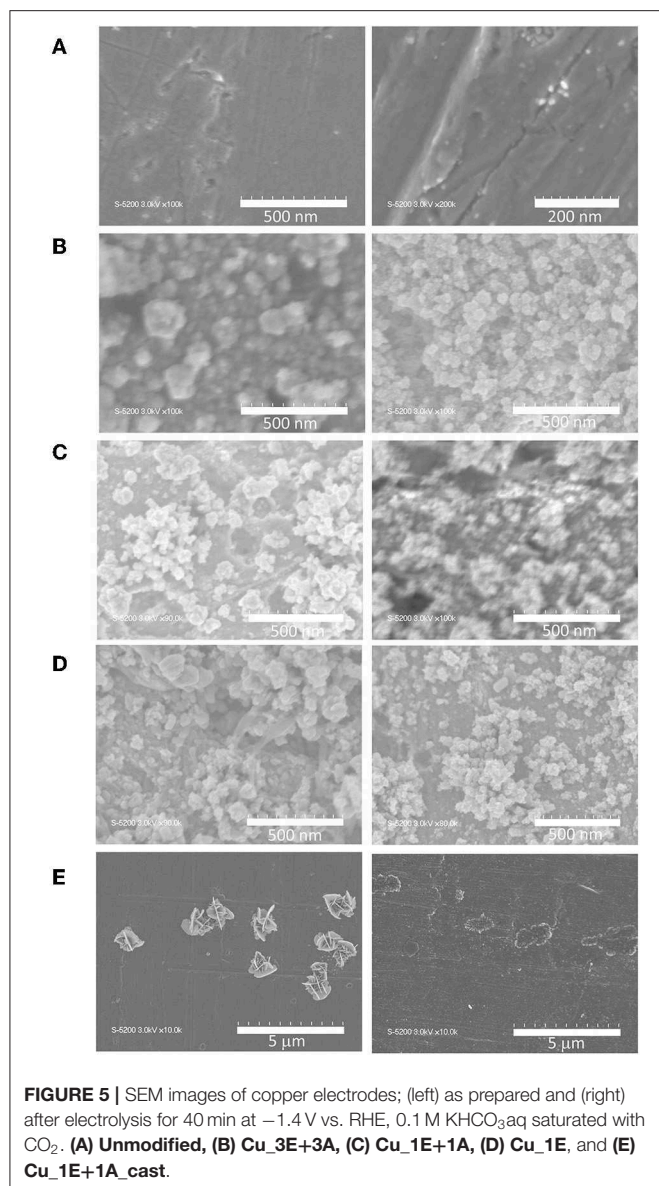
the majority of the grain structure was composed of copper. In **Cu_1E+1A_cast**, the organic moieties seemed to be aggregated to form massive crystals that inhibited the Pb deposition process on the electrode surface.

CO₂ REDUCTION

The formation of carbon products by CO₂ reduction at −1.4 V (vs. reversible hydrogen electrode, RHE, solution resistance uncorrected, **Figure 7**) showed that **Cu_3E+3A** had the highest amount of carbonaceous product formation. The products demonstrate two remarkable effects of modification: (i) ethylene formation was enhanced by anodic scanning in the presence of the ethynyl precursors; (ii) only the **Cu_3E+3A** electrode exhibited improved methane formation as a result of modification, while the other electrodes appeared to compensate for ethylene formation with methane formation.

Comparison of the Faradaic efficiency (**Figure 8**) reveals that the high CO₂ reduction performance of **Cu_3E+3A** did not result simply from an increase in total current with increasing roughness of the electrode surface. Besides the increase in methane and ethylene formation, **Cu_3E+3A** exhibited remarkably low hydrogen production, which is undesirable for the proton-consuming side reaction. Also, the control experiment under argon only bore hydrogen from **Cu_3E+3A** at the potential range, showing that the modified organics were not the source of hydrocarbons (**Figure S6**).

The linear sweep voltammetry (LSV) curves (**Figure 9**) of the electrodes provide additional information on reaction selectivity. At low current densities (−0.4 to −0.8 V), the current ratio appears to largely depend on the roughness factor. Further reducing the negative potential to under −1.0 V resulted in similar current densities for all electrodes (ca. −2 mAcm^{−2}),

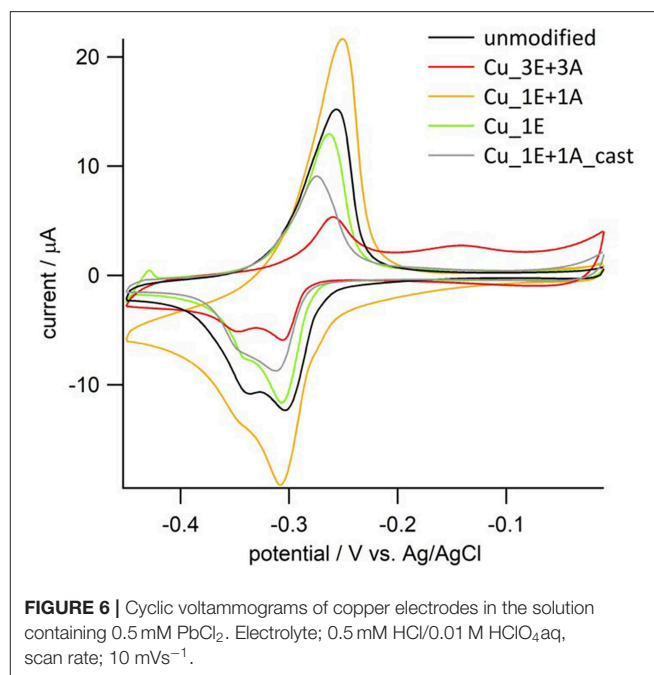


despite observed differences in the roughness factor. At high current densities, the thickness of the CO₂ and proton diffusion layer increased beyond the scale of the thickness of the deposited surface structures. Therefore, the reaction is limited by the transportation properties. The polarization involves multiple electrochemical processes. By incrementally increasing the potential, the onset of CO₂ reduction to CO and hydrogen evolution was observed to first emerge at approx. -0.4 V, and the reduction of adsorbed CO into hydrocarbons was further enhanced when the potential was under -1.0 V. The current in Cu_3E+3A displayed slow increments despite of a relatively positive current onset, indicating that significant CO adsorption results in a current drop until the potential reaches -1.0 V, as CO₂ reduction is significantly more efficient than H₂ evolution. Thereafter, the current rapidly increased below -1.0 V as the adsorbed CO was removed through further

TABLE 1 | Roughness factors of copper electrodes.

	Unmodified	Cu_3E+3A	Cu_1E+1A	Cu_1E	Cu_1E+1A_cast
	1.0	1.8	4.0	3.7	1.4
After EL ^a	0.9	1.9	4.3	3.9	1.7

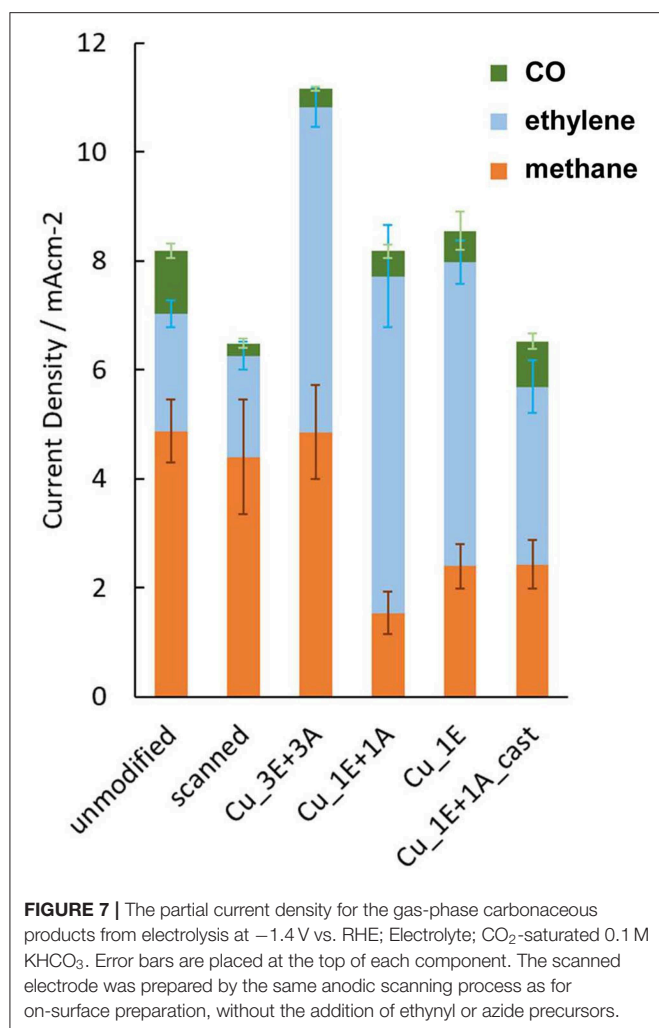
^aElectrolysis was carried out for 50 min from -1.0 to -1.4 V vs. RHE with a stepwise increment of -0.1 V in every 10 min.



reduction into hydrocarbons followed by dissociation, consistent with the potential dependence of Faradaic efficiency for H₂ and CO (Figure 8).

The effect on CO₂ reduction is influenced by how the organic moieties contact with the copper surface. In repeated cast modifications of the polished Cu electrode, the total current density was not observed to decrease; however, the formation of carbonaceous products decreased depending on the number of times the copper electrode was subjected to the cast process and was even surpassed by hydrogen production (Figure 10). The casting of molecular triazole typically forms densely packed crystalline structures that inhibit the adsorption of CO₂ on the surface. Conversely, this is not the case for H₂ production, as H₂ evolution requires significantly smaller surface vacancies to adsorb H atoms, and it may even be possible on the adsorbed organic molecules.

An ethylene increase was observed for the electrodes that were subjected to repetitive anodic scanning in the presence of the ethynyl precursor. The existence of the insoluble copper(I) acetylide intermediate on the surface is important for copper reorganization. This observed trend is similar to the high ethylene formation efficiency observed for nanostructured CO₂-reduction catalysts that are prepared by the formation of an insoluble copper oxide layer on the surface followed by reduction to Cu(0) (Kas et al., 2014; Ren et al., 2015; Dutta



et al., 2016; Handoko et al., 2016; Mistry et al., 2016; Mandal et al., 2018). During anodization in the absence of the ethynyl precursor (“scanned” in **Figure 7**), CO₂ reduction resulted in a decrease in the efficiency of ethylene formation. Continuous dissolution of copper into acetonitrile, without the precursor, may remove the copper atoms at the defect site of the copper crystal facet.

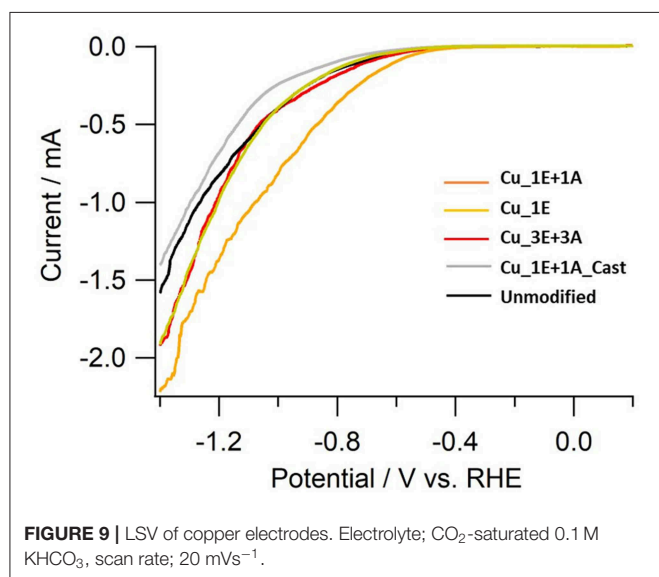
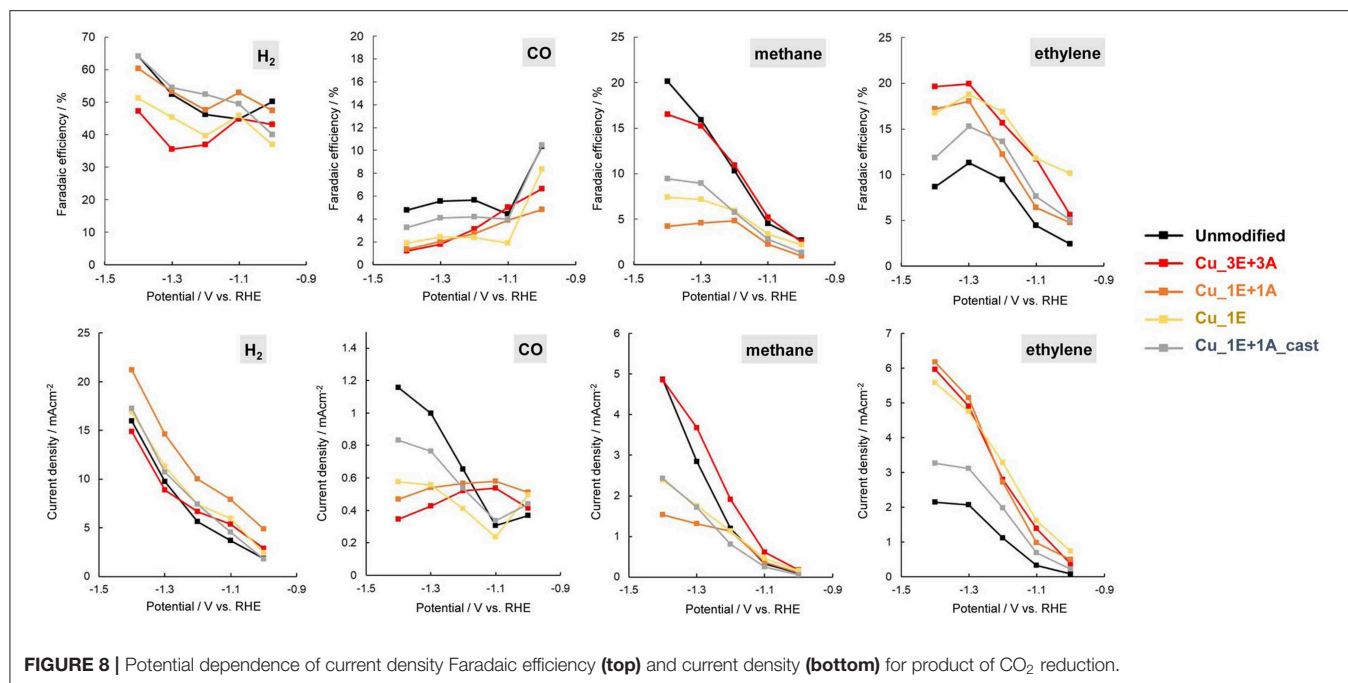
In the majority of Cu electrocatalytic processes, there is a trade-off in the efficiency of methane and ethylene selectivity. Additionally, the pH of the electrolyte influences the ratio of methane and ethylene, as the reduction process is related to competition of the dimerization of the adsorbed CO and the proton-coupled reduction (Schouten et al., 2011, 2013; Huang et al., 2017). The potential dependence of the ethylene/methane ratio also shows that methane formation is dominant with increased current density, as the reduction rate surpasses CO dimerization. Further increasing the current density results in an increase in pH on the surface due to H⁺ consumption, resulting in dominant H₂ production through H₂O reduction because CO₂ is not stable in alkaline media (Singh et al., 2016). This trend appears to hold true in the case of **Cu_1E+1A** and **Cu_1E**, as the total CO₂ reduction efficiency remained at a similar level to that

of the unmodified electrode. In **Cu_3E+3A**, both methane and ethylene increased with remarkably low hydrogen production. Hence, the organic layers play a role in increasing the total CO₂ reduction efficiency.

Stirring the electrolyte solution also changes the transport conditions. When stirring of the solution was stopped (**Figure 11**), the amount of dissolved components in the electrolyte (most likely formate) decreased for both the unmodified and **Cu_3E+3A** electrodes. Hydrogen was observed to increase for the unmodified electrode, but with the **Cu_3E+3A** electrode, the decrease of the soluble product content appeared to be compensated for by hydrocarbon formation, especially methane. Under a high current-flow condition without stirring, a pH increase at the electrode surface was observed to occur, as every electron transfer was accompanied by a proton transfer. Furthermore, the depletion of CO₂ was more severe for two reasons: (i) CO₂ possesses a lower diffusion coefficient than H⁺, and (ii) CO₂ transforms to HCO₃⁻ in basic media. The suppression of hydrogen evolution by modification of the electrode appears to result from the preference of CO₂ reduction and adsorption over the reduction of H₂O. CO₂ selectivity is affected by the competition between CO₂ reduction and proton reduction forming surface-adsorbed H, and the latter process tends to lead to the formation of H₂ and formate. Several recent reports have demonstrated that hydrophobic modification of the surface improves the supply of CO₂ relative to H⁺, which leads to better selectivity to CO and hydrocarbons (Buckley et al., 2019; Li et al., 2019). Moreover, the three-way triazole moiety was reported to have specific affinity in MOF CO₂ storage (Wang et al., 2013). In our case, the introduction of the organic layer made the surface more hydrophobic (**Figure S7**). The presence of the organic layer seems to create a CO₂-rich environment on the electrode surface, possibly by improved proton transfer and better CO₂ affinity with the layer than with the bare electrode surface.

CONCLUSIONS

A novel method has been designed to modify the surface of a metal electrode to enhance surface catalytic activity by anodization. The metal-organic contact structure formed offers unique properties over those of traditional cathodes prepared *via* the cast method by inducing a thin layer of organic moieties that are accessible to surface copper atoms. The influence of the modified electrode on CO₂ reduction reveals that the contact surface has a preference toward CO₂ reduction over H₂ evolution, contrary to the observed results from surfaces modified by the cast method. The organic layer appears to enhance the environment to achieve improved CO₂ affinity and proton transport ability at the surfaces of the copper atoms. The re-organization of copper atoms upon modification did influence CO₂ reduction selectivity, as in copper oxide-derived electrocatalysis. However, this property is not the sole factor governing the observed CO₂ reduction selectivity, because a large total CO₂ reduction efficiency and high methane formation are observed, even at low potentials. The method herein

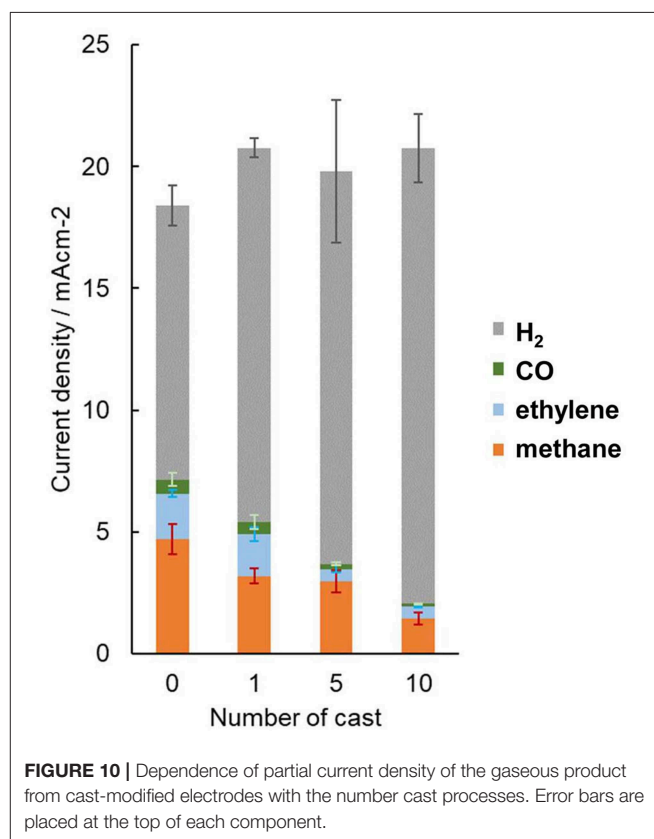


can readily introduce various types of organic substituents to the organic-open metal contact surface. Studies are underway to investigate controlling the CO₂ reduction based on the discussion in this report. Furthermore, the introduction of an organic functional center, such as ligands and dyes, would allow for CO₂ reduction with cooperated activation or light-driven functionality.

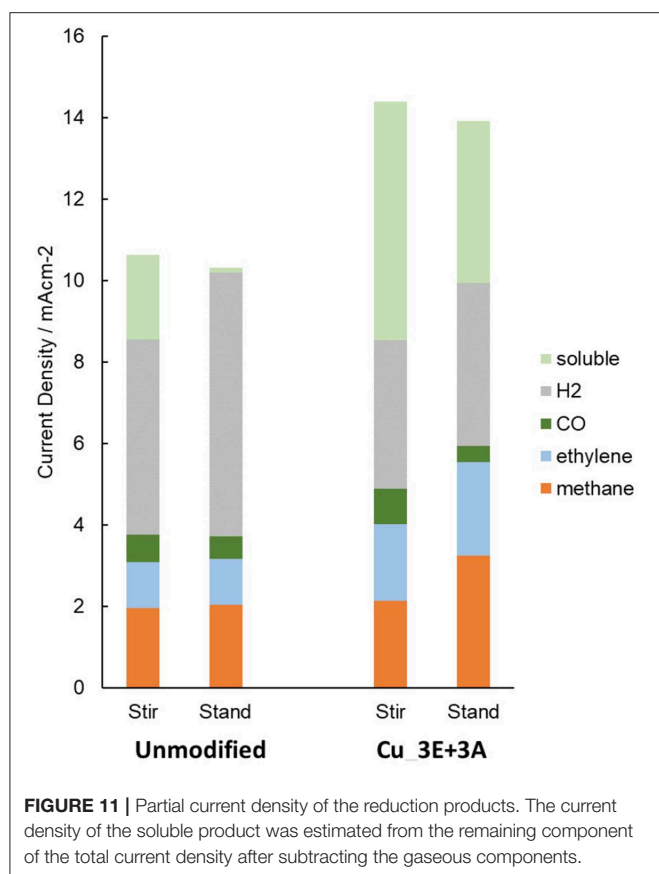
METHODS

Electrode Modification

A disc copper electrode (3 mm ϕ) was made from the cross-section of a polycrystalline rod embedded in a glass



tube and polished with Bicalox0.05CR (0.05 μ m alumina abrasive). Modification was performed in 5 mL electrolyte (0.1 M ⁿBu₄NPF₆-acetonitrile) containing ethynyl (6.6 mM) and azide (6.6 mM) precursors under an argon atmosphere. A potential



scan was repeated 15 times (from -0.2 to -1.0 V vs. Ag/Ag⁺, 0.1 Vs⁻¹) using an ALS 650D potentiostat, followed by washing with acetonitrile. For cast modification, 0.7 μ L of acetonitrile solution containing 1-benzyl-4-phenyl-1,2,3-triazole (4.3 mM) was dropped on the copper disc and air-dried. Modified copper substrates for XPS and SEM measurements were prepared using 5 mm square copper foil instead of copper discs.

Characterization of Surface Structure

SEM images were collected with a Hitachi FE-SEM S-5200. XPS data were collected using a KRATOS ESCA 3400 with an Al-K α source. Double-layer capacitance was measured in CO₂ saturated 0.1 M KHCO₃aq on the basis of the current dependence upon the potential scan rate in the region of -0.6 V to -0.7 V vs. Ag/AgCl. UPD was achieved by immersing the modified electrode in electrolyte-containing lead salt (0.5 mM PbCl₂, 0.5 mM HCl/ 10 mM HClO₄aq, scan rate; 10 mVs⁻¹).

CO₂ Reduction

The CO₂ reduction activity on copper electrodes was investigated in CO₂-saturated 0.1 M KHCO₃aq (pH 6.8). The three-electrode

setup was connected to a potentiostat (ALS 650D). Ag/AgCl was used as a reference electrode, and Pt mesh was used as the counter electrode. The applied potential was converted to RHE according to the equation $E_{RHE} = E_{Ag/AgCl} + 0.197$ V + $0.0591 \times$ pH.

The experiments were performed in a two-compartment cell. A copper working electrode and Ag/AgCl electrode were placed in the gas-tight cathodic compartment. It was separated from the open anodic compartment, which was equipped with a Pt mesh counter electrode, by a 10 mm ϕ ion-exchange membrane (SelemionTM AMV). Electrolysis was performed for 10 min with stirring (ca. 600 rpm), without additional supply of CO₂. Depletion of CO₂ by electrolysis did not exceed a few % of the amount of CO₂ in solution (34 mM, 6.2 mL), which is estimated from the charge flow (typically 1 C). For the quantification of gaseous products, 0.1 mL of gas product was collected from the head space (9.9 mL) of the gas-tight compartment and introduced in a gas chromatograph (Shimadzu-2010) equipped with a 2.0 m \times 1.0 mm ID column packed with SHINCARBON ST and a BID-2010 detector. Copper electrodes were first cathodized at -1.6 V vs. Ag/AgCl for 1 h to remove weakly physisorbed materials and reduce oxidized copper species prior to the collection of CO₂RR products. The current density was calculated according to the geometric area of the Cu electrode (3 mm ϕ). CO₂ reduction data are provided as averages from at least three separately prepared electrodes.

AUTHOR CONTRIBUTIONS

SK, KK, and TM contributed the overall concept of the study. SK and RT developed the experimental apparatus for electrolysis. RT and RI performed the experiments and analysis of the collected data. All authors contributed to manuscript revision and read and approved the submitted version.

FUNDING

This work was supported by JSPS KAKENHI Grant Number: JP16K05723.

ACKNOWLEDGMENTS

The authors acknowledge Dr. M. Maeda for support in SEM image collection and Dr. H. Dote for assistance in XPS measurements. We thank the Edanz Group (www.edanzediting.com/ac) for editing a draft of this manuscript.

SUPPLEMENTARY MATERIAL

The Supplementary Material for this article can be found online at: <https://www.frontiersin.org/articles/10.3389/fchem.2019.00860/full#supplementary-material>

REFERENCES

Abrantes, L., Fleischmann, M., Hill, I., Peter, L., Mengoli, M., and Zotti, G. (1984). An investigation of Cu(I) acetylide films on Cu electrodes: Part I. Electrochemical and Raman spectroscopic

analysis of the film formation. *J. Electroanal. Chem. Interfacial Electrochem.* 164, 177–187. doi: 10.1016/S0022-0728(84)0238-7

Ahn, S., Klyukin, K., Wakeham, R. J., Rudd, J. A., Lewis, A. R., Alexander, S., et al. (2018). Poly-amide modified copper foam electrodes for enhanced

- electrochemical reduction of carbon dioxide. *ACS Catal.* 8, 4132–4142. doi: 10.1021/acscatal.7b04347
- Ahrland, S. (1982). Solvation and complex formation. Competing and cooperative processes in solution. *Pure Appl. Chem.* 54, 1451–1468. doi: 10.1351/pac198254081451
- Bandyopadhyay, K., Patil, V., Sastry, M., and Vijayamohan, K. (1998). Effect of geometric constraints on the self-assembled monolayer formation of aromatic disulfides on polycrystalline gold. *Langmuir* 14, 3808–3814. doi: 10.1021/la980088i
- Buckley, A., Lee, M., Cheng, T., Kazantsev, R. V., Larson, D. M., Goddard, W. A., et al. (2019). Electrocatalysis at organic-metal interfaces: identification of structure-reactivity relationships for CO₂ reduction at modified Cu surfaces. *J. Am. Chem. Soc.* 141, 7355–7364. doi: 10.1021/jacs.8b13655
- Chisholm, R., Parkin, J. D., Smith, A. D., and Hahner, G. (2016). Isothiourea-mediated organocatalytic michael addition-lactonization on a surface: modification of SAMs on silicon oxide substrates. *Langmuir* 32, 3130–3138. doi: 10.1021/acs.langmuir.5b04686
- Collman, J. P., Devaraj, N. K., Eberspacher, T. P. A., and Chidsey, C. E. D. (2006). Mixed azide-terminated monolayers: a platform for modifying electrode surfaces. *Langmuir* 22, 2457–2464. doi: 10.1021/la052947q
- Dutta, A., Rahaman, M., Luedi, N. C., Mohos, M., and Broekmann, P. (2016). Morphology matters: tuning the product distribution of CO₂ electroreduction on oxide-derived Cu foam catalysts. *ACS Catal.* 6, 3804–3814. doi: 10.1021/acscatal.6b00770
- Feaster, J. T., Shi, C., Cave, E. R., Hatsukade, T., Abram, D. N., Kuhl, K. P., et al. (2017). Understanding selectivity for the electrochemical reduction of carbon dioxide to formic acid and carbon monoxide on metal electrodes. *ACS Catal.* 7, 4822–4827. doi: 10.1021/acscatal.7b00687
- Feng, Y., Dionne, E. R., Toader, V., Beaudoin, G., and Badia, A. (2017). Odd-even effects in electroactive self-assembled monolayers investigated by electrochemical surface plasmon resonance and impedance spectroscopy. *J. Phys. Chem. C* 121, 24626–24640. doi: 10.1021/acs.jpcc.7b08053
- Gattrell, M., Gupta, N., and Co, A. (2006). A review of the aqueous electrochemical reduction of CO₂ to hydrocarbons at copper. *J. Electroanal. Chem.* 594, 1–19. doi: 10.1016/j.jelechem.2006.05.013
- Gong, M., Cao, Z., Liu, W., Nichols, E. M., Smith, P. T., Derrick, J. S., et al. (2017). Supramolecular porphyrin cages assembled at molecular-materials interfaces for electrocatalytic CO reduction. *ACS Cent. Sci.* 3, 1032–1040. doi: 10.1021/acscentsci.7b00316
- Gunathunge, C. M., Li, X., Li, J., Hicks, R. P., Ovalle, V. J., and Waegle, M. M. (2017). Spectroscopic observation of reversible surface reconstruction of copper electrodes under CO₂ reduction. *J. Phys. Chem. C* 121, 12337–12344. doi: 10.1021/acs.jpcc.7b03910
- Gupta, N., Gattrell, M., and MacDougall, B. (2006). Calculation for the cathode surface concentrations in the electrochemical reduction of CO₂ in KHCO₃ solutions. *J. Appl. Electrochem.* 36, 161–172. doi: 10.1007/s10800-005-9058-y
- Handoko, A. D., Ong, C. W., Huang, Y., Lee, Z. G., Lin, L., Panetti, G. B., et al. (2016). Mechanistic insights into the selective electroreduction of carbon dioxide to ethylene on Cu₂O-derived copper catalysts. *J. Phys. Chem. C* 120, 20058–20067. doi: 10.1021/acs.jpcc.6b07128
- Hori, Y., Kikuchi, K., Murata, A., and Suzuki, S. (1986). Production of methane and ethylene in electrochemical reduction of carbon dioxide at copper electrode in aqueous hydrogencarbonate solution. *Chem. Lett.* 15, 897–898. doi: 10.1246/cl.1986.897
- Hori, Y., Kikuchi, K., and Suzuki, S. (1985). Production of CO and CH₄ in electrochemical reduction of CO₂ at metal electrodes in aqueous hydrogencarbonate solution. *Chem. Lett.* 14, 1695–1698. doi: 10.1246/cl.1985.1695
- Hori, Y., Takahashi, I., Koga, O., and Hoshi, N. (2003). Electrochemical reduction of carbon dioxide at various series of copper single crystal electrodes. *J. Mol. Cat. A* 199, 39–47. doi: 10.1016/S1381-1169(03)00016-5
- Hori, Y., Takahashi, R., Yoshinami, Y., and Murata, A. (1997). Electrochemical reduction of CO at a copper electrode. *J. Phys. Chem. B* 101, 7075–7081. doi: 10.1021/jp970284i
- Huang, Y., Handoko, A. D., Hirunsit, P., and Yeo, B. S. (2017). Electrochemical reduction of CO₂ using copper single-crystal surfaces: effects of CO* coverage on the selective formation of ethylene. *ACS Catal.* 7, 1749–1756. doi: 10.1021/acscatal.6b03147
- Jeon, H. S., Kunze, S., Scholten, F., and Roldan Cuenya, B. (2018). Prism-shaped Cu nanocatalysts for electrochemical CO₂ reduction to ethylene. *ACS Catal.* 8, 531–535. doi: 10.1021/acscatal.7b02959
- Kas, R., Kortlever, R., Milbrat, A., Koper, M. T. M., Mul, G., and Baltrusaitis, J. (2014). Electrochemical CO₂ reduction on Cu₂O-derived copper nanoparticles: controlling the catalytic selectivity of hydrocarbons. *Phys. Chem. Chem. Phys.* 16, 12194–12201. doi: 10.1039/C4CP01520G
- Kim, D., Kley, C. S., Li, Y., and Yang, P. (2017). Copper nanoparticle ensembles for selective electroreduction of CO₂ to C₂-C₃ products. *Proc. Natl. Acad. Sci. U.S.A.* 114, 10560–10565. doi: 10.1073/pnas.1711493114
- Kuhl, K. P., Cave, E. R., Abram, D. N., and Jaramillo, T. F. (2012). New insights into the electrochemical reduction of carbon dioxide on metallic copper surfaces. *Energy Environ. Sci.* 5, 7050–7059. doi: 10.1039/c2ee21234j
- Li, A., Cao, Q., Zhou, G., Schmidt, B. V. K., Zhu, W., Yuan, X., et al. (2019). Three-phase photocatalysis for the enhanced selectivity and activity of CO₂ reduction on a hydrophobic surface. *Angew. Chem. Int. Ed.* 58, 14549–14555. doi: 10.1002/anie.201908058
- Li, C. W., and Kanan, M. W. (2012). CO₂ Reduction at low overpotential on Cu electrodes resulting from the reduction of thick Cu₂O films. *J. Am. Chem. Soc.* 134, 7231–7234. doi: 10.1021/ja3010978
- Long, R., Li, Y., Liu, Y., Chen, S., Zheng, X., Gao, C., et al. (2017). Isolation of Cu atoms in Pd lattice: forming highly selective sites for photocatalytic conversion of CO₂ to CH₄. *J. Am. Chem. Soc.* 139, 4486–4492. doi: 10.1021/jacs.7b00452
- Luna, P. D., Quintero-Bermudez, R., Dinh, C. D., Ross, M. B. R., Bushuyev, O. S., Todorović, P., et al. (2018). Catalyst electro-redeposition controls morphology and oxidation state for selective carbon dioxide reduction. *Nat. Catal.* 1, 103–110. doi: 10.1038/s41929-017-0018-9
- Ma, M., Djanashvili, K., and Smith, W. A. (2015). Selective electrochemical reduction of CO₂ to CO on CuO-derived Cu nanowires. *PCCP* 17, 20861–20867. doi: 10.1039/C5CP03559G
- Ma, S., Sadakiyo, M., Heima, M., Luo, R., Haasch, R. T., Gold, J. I., et al. (2017). Electroreduction of carbon dioxide to hydrocarbons using bimetallic Cu–Pd catalysts with different mixing patterns. *J. Am. Chem. Soc.* 139, 47–50. doi: 10.1021/jacs.6b10740
- Mandal, L., Yang, K. R., Motapothula, M. R., Ren, D., Lobaccaro, P., Patra, A., et al. (2018). Investigating the role of copper oxide in electrochemical CO₂ reduction in real time. *ACS Appl. Mater. Interfaces* 10, 8574–8584. doi: 10.1021/acscami.7b15418
- Mistry, H., Varela, A. S., Bonifacio, C. S., Zegkinoglou, I., Sinev, I., Choi, Y., et al. (2016). Highly selective plasma-activated copper catalysts for carbon dioxide reduction to ethylene. *Nat. Commun.* 7, 12123. doi: 10.1038/ncomms12123
- Ooka, H., Figueiredo, M. C., and Koper, M. T. M. (2017). Competition between hydrogen evolution and carbon dioxide reduction on copper electrodes in mildly acidic media. *Langmuir* 33, 9307–9313. doi: 10.1021/acs.langmuir.7b00696
- Peterson, A. A., and Nørskov, J. K. (2012). Activity descriptors for CO₂ electroreduction to methane on transition-metal catalysts. *J. Phys. Chem. C* 116, 251–258. doi: 10.1021/jz201461p
- Qiu, Y., Zhong, H., Zhang, T., Xu, W., Li, X., and Zhang, H. (2017). Copper electrode fabricated via pulse electrodeposition: toward high methane selectivity and activity for CO₂ electroreduction. *ACS Catal.* 7, 6302–6310. doi: 10.1021/acscatal.7b00571
- Ren, D., Deng, Y., Handoko, A. D., Chen, C. S., Malkhandi, S., and Yeo, B. S. (2015). Selective electrochemical reduction of carbon dioxide to ethylene and ethanol on Copper(I) oxide catalysts. *ACS Catal.* 5, 2814–2821. doi: 10.1021/cs502128q
- Reske, R., Mistry, H., Beharfarid, F., Cuenya, B. R., and Strasser, P. (2014). Particle size effects in the catalytic electroreduction of CO₂ on Cu nanoparticles. *J. Am. Chem. Soc.* 136, 6978–6986. doi: 10.1021/ja500328k
- Schoenbaum, C. A., Schwartz, D. K., and Medlin, J. W. (2014). Controlling the surface environment of heterogeneous catalysts using self-assembled monolayers. *Acc. Chem. Res.* 47, 1438–1445. doi: 10.1021/ar500029y
- Schouten, K. J. P., Gallent, E. P., and Koper, M. T. M. (2013). Structure sensitivity of the electrochemical reduction of carbon monoxide on copper single crystals. *ACS Catal.* 3, 1292–1295. doi: 10.1021/cs4002404
- Schouten, K. J. P., Kwon, Y., van der Ham, C. J. M., Qin, Z., and Koper, M. T. M. (2011). A new mechanism for the selectivity to C₁ and C₂ species in the

- electrochemical reduction of carbon dioxide on copper electrodes. *Chem. Sci.* 2, 1902–1909. doi: 10.1039/c1sc00277e
- Schouten, K. J. P., Qin, Z., Gallent, E. P., and Koper, M. T. M. (2012). Two pathways for the formation of ethylene in CO reduction on single-crystal copper electrodes. *J. Am. Chem. Soc.* 134, 9864–9867. doi: 10.1021/ja302668n
- Singh, M. R., Kwon, Y., Lum, Y., Ager, J. W., and Bell, A. T. (2016). Hydrolysis of electrolyte cations enhances the electrochemical reduction of CO₂ over Ag and Cu. *J. Am. Chem. Soc.* 138, 13006–13012. doi: 10.1021/jacs.6b07612
- Tang, W., Peterson, A. A., Varela, A. S., Jovanov, Z. P., Bech, L., Durand, W. J., et al. (2011). The importance of surface morphology in controlling the selectivity of polycrystalline copper for CO₂ electroreduction. *Phys. Chem. Chem. Phys.* 14, 76–81. doi: 10.1039/C1CP22700A
- Varela, A. S., Kroschel, M., Reier, T., and Strasser, P. (2016). Controlling the selectivity of CO₂ electroreduction on copper: the effect of the electrolyte concentration and the importance of the local pH. *Catal. Today* 260, 8–13. doi: 10.1016/j.cattod.2015.06.009
- Wang, X., Li, P., Chen, Y., Zhang, Q., Zhang, H., Chan, X. X., et al. (2013). A rationally designed nitrogen-rich metal-organic framework and its exceptionally high CO₂ and H₂ uptake capability. *Sci. Rep.* 3:1149. doi: 10.1038/srep01149
- Xie, M. S., Xia, B. Y., Li, Y., Yan, Y., Yang, Y., Sun, Q., et al. (2016). Amino acid modified copper electrodes for the enhanced selective electroreduction of carbon dioxide towards hydrocarbons. *Energy Environ. Sci.* 9, 1687–1695. doi: 10.1039/C5EE03694A
- Zhang, F., Sheng, T., Tian, N., Liu, L., Xiao, C., Lu, B., et al. (2017). Cu overlayers on tetrahedral Pd nanocrystals with high-index facets for CO₂ electroreduction to alcohols. *Chem. Commun.* 53, 8085–8088. doi: 10.1039/C7CC04140C
- Zhang, Y., Sethuraman, V., Michalsky, R., and Peterson, A. A. (2014). Competition between CO₂ reduction and H₂ evolution on transition-metal electrocatalysts. *ACS Catal.* 4, 3742–3748. doi: 10.1021/cs5012298
- Zhao, J., Sun, L., Canepa, S., Sun, H., Yesibolati, M. N., Sherburne, M., et al. (2017). Phosphate tuned copper electrodeposition and promoted formic acid selectivity for carbon dioxide reduction. *J. Mater. Chem. A* 5, 11905–11916. doi: 10.1039/C7TA01871A

Conflict of Interest: The authors declare that the research was conducted in the absence of any commercial or financial relationships that could be construed as a potential conflict of interest.

Copyright © 2019 Igarashi, Takeuchi, Kubo, Mizuta and Kume. This is an open-access article distributed under the terms of the Creative Commons Attribution License (CC BY). The use, distribution or reproduction in other forums is permitted, provided the original author(s) and the copyright owner(s) are credited and that the original publication in this journal is cited, in accordance with accepted academic practice. No use, distribution or reproduction is permitted which does not comply with these terms.